

## ON DIFFUSION OF CHEMICALLY REACTIVE SPECIES IN A CONVECTIVE FLOW PAST AN INCLINED PLATE WITH VARIABLE SURFACE TEMPERATURE AND VARIABLE MASS DIFFUSION

J.D. KIRUBAVATHI and G. PALANI\*

Department of Mathematics, Dr. Ambedkar Govt. Arts College  
Chennai 600 039, Tamil Nadu, INDIA  
E-mail: gpalani32@yahoo.co.in

A numerical solution of a transient natural convection flow past a semi-infinite inclined plate under the combined buoyancy effects of heat and mass transfer along with chemical reaction is presented herewith. The governing boundary layer equations for the above flow problem for a first order homogeneous chemical reaction are set up and non-dimensionalised. An implicit finite difference method is employed to solve the unsteady, non-linear, integro and coupled partial differential equation. Numerical results are presented for various parameters occurring in the problem. The unsteady velocity, temperature and concentration profiles, local and average skin friction, Nusselt number and Sherwood number are studied for both a generative and destructive reaction.

**Key words:** chemically reactive species, finite-difference method, inclined plate, skin friction and Nusselt number.

### 1. Introduction

In many engineering processes, heat and mass transfer take place simultaneously. The common example of heat and mass transfer is the evaporation of lake water into the wind flowing over it. In some cases, mass transfer is predominant and heat transfer may be negligible and in other cases both remain equally predominant. Mass transfer will occur as long as there is a difference in concentration of some chemical species in the mixture. Hence the concentration gradient acts as a driving potential in mass transfer just as the temperature gradient does in heat transfer. Mass diffusion occurs in liquids and solids as well as in gases. Examples of diffusion in gases, liquids and solids respectively, include nitrous oxide from an automobile exhaust in air, dissolved oxygen in water and helium in Pyrex.

Theoretical consideration of combined thermal and mass transfer from a vertical plate to gases under natural convection has been studied by Somers [1]. To solve the steady state problem for uniform surface temperature and diffusing species concentration, an integral method has been employed. Mathers *et al.* [2] formulated the same problem by using boundary layer approximation and omitting the interial terms in the momentum equation. Wilcox [3] studied the problem of simultaneous heat and mass transfer using the integral method. Gebhart and Pera [4] observed the steady state natural convection on a vertical plate with variable surface temperature and variable mass diffusion. The boundary layer equations were solved by using similarity variables. Callahan and Marner [5] solved the problem of transient free convection with mass transfer on an isothermal vertical flat plate. An explicit finite difference scheme was used to solve transient boundary layer equations. Ekambavannan and Ganesan [6] studied an unsteady natural convection flow along an inclined plate with variable surface temperature and mass diffusion. They solved the boundary layer equations using an implicit finite difference scheme.

Many practical diffusion operations involve the molecular diffusion of a species in the presence of chemical reaction taking place either within or at the boundary. There are two types of chemical reactions

---

\* To whom correspondence should be addressed

namely: a homogenous reaction and a heterogeneous reaction. Species transfer by diffusion may be influenced by a homogenous chemical reaction just as heat diffusion may be influenced by an internal source of energy. When foreign mass is present in air or water, some chemical reaction may take place, e.g., air and benzene react chemically together. In recent years, the requirements of modern technology have stimulated interest in fluid flow studies, which involve the interaction of several phenomena. One such study is related to the diffusion of a chemically reactive species in a laminar boundary layer flow over an inclined plate with combined heat and mass transfer. For example, this type of problem can arise in electroplating. The phenomenon of heat and mass transfer is encountered in chemical process industries such as food processing and polymer production.

A few representative fields of interest in which combined heat and mass transfer along with chemical reaction play an important role in chemical process industries such as food processing and polymer production. For example, formation of smog is a first order homogeneous chemical reaction. Consider the emission of  $NO_2$  from automobiles and other smoke-stacks.  $NO_2$  reacts chemically in the atmosphere with unburned hydrocarbons (aided by sunlight) and produces peroxyacetyl nitrate, which forms an envelope of what is termed as petrochemical smog. Chambre and Young [7] analysed the problem of first order chemical reactions in the neighborhood of a flat plate for destructive and generative reactions. Das *et al.* [8] presented an exact solution to the flow due to impulsive motion of an infinite vertical plate in the presence of species concentration and first order chemical reaction for uniform heat flux at the plate. Das *et al.* [9] presented an exact solution to the flow of a viscous incompressible fluid past an impulsively started vertical plate in the presence of mass transfer and first order chemical reaction. A finite-difference solution for a transient natural convective flow of an incompressible viscous fluid past an impulsively started semi-infinite plate with a constant heat flux and mass diffusion was presented by Muthucumaraswamy and Ganesan [10] by taking into account a homogenous chemical reaction of the first order. Muthucumaraswamy and Ganesan [11] also presented an exact solution of the problem of a flow past an impulsively started infinite vertical plate with a variable temperature and uniform mass diffusion by taking into account a homogenous chemical reaction of the first order. An approximate numerical solution for a steady MHD laminar-boundary layer flow over an accelerating vertical surface with suction or injection in the presence of a species concentration and mass diffusion was obtained by Anjali Devi and Kandasamy [12] by using R.K. Gill's method. A theoretical solution of the problem of a flow past an impulsively started infinite vertical plate in the presence of a uniform heat flux and variable mass diffusion was presented by Muthucumaraswamy and Kulandaivel [13] by considering a homogenous chemical reaction of the first order. Loganathan *et al.* [14] studied the first-order chemical reaction on a moving semi-infinite vertical plate in the presence of an optically thin gray gas, using a finite-difference method.

In the present study, we consider the effects of mass transfer on the flow past a semi-infinite inclined plate with chemical reaction. No analysis seems to have been presented for transient natural convection flow past a semi-infinite inclined plate with chemical reaction. The main reason for the lack of studies on this problem is due to difficult mathematical and numerical procedures in dealing with the non-similar boundary layers. The conservation equations of an unsteady laminar boundary layer are first transformed into a non-dimensional form and their solutions are then obtained by an efficient implicit finite difference scheme of Crank-Nicolson type.

## 2. Mathematical analysis

A two-dimensional transient laminar natural convection flow of a viscous incompressible fluid past a semi-infinite inclined plate with wall temperature  $T_w(x) = T_w + ax^n$  and concentration on the surface  $C'_w(x) = C'_\infty + bx^m$  is considered. The  $x$ -axis is taken along the plate and  $y$ -axis is taken along upward normal to the plate,  $\theta$  is the angle of inclination of the plate with the horizontal. The effect of viscous dissipation is assumed to be neglected in the energy equation. It is also assumed that there exists a homogeneous first order chemical reaction between the fluid and species concentration. But here we assume that the level of species concentration is very low and hence heat generated during chemical reaction can be neglected. In this reaction, the reactive component given off by the surface occurs only in a very dilute form. Hence any

convective mass transfers to or from the surface due to net viscous dissipation effects in the energy equation are assumed to be negligible. The surrounding fluid which is at rest has a temperature  $T$  and concentration  $C$ . The governing boundary layer equation of mass, momentum, energy and species concentration for free convective flows under Boussinesq's approximation are as follows

$$\frac{\partial u}{\partial x} + \frac{\partial v}{\partial y} = 0, \tag{2.1}$$

$$\begin{aligned} \frac{\partial u}{\partial t'} + u \frac{\partial u}{\partial x} + v \frac{\partial u}{\partial y} = g\beta \cos \phi \frac{\partial}{\partial x} \int_y^\infty (T' - T_\infty') dy + \sin \phi (T' - T_\infty') + \\ + g\beta^* \cos \phi \frac{\partial}{\partial x} \int_y^\infty (C' - C_\infty') dy + \sin \phi (C' - C_\infty') + v \frac{\partial^2 u}{\partial y^2}, \end{aligned} \tag{2.2}$$

$$\frac{\partial T'}{\partial t'} + u \frac{\partial T'}{\partial x} + v \frac{\partial T'}{\partial y} = \alpha \frac{\partial^2 T'}{\partial y^2}, \tag{2.3}$$

$$\frac{\partial C'}{\partial t'} + u \frac{\partial C'}{\partial x} + v \frac{\partial C'}{\partial y} = D \frac{\partial^2 C'}{\partial y^2} - K' C'. \tag{2.4}$$

The initial and boundary conditions are

$$\begin{aligned} t' \leq 0: \quad u = 0, \quad v = 0, \quad T' = T_\infty', \quad C' = C_\infty' \quad \text{for all } x \quad \text{and } y, \\ t' > 0: \quad u = 0, \quad v = 0, \quad T' = T_\infty' + ax^n, \quad C' = C_\infty' + bx^m \quad \text{at } y = 0, \\ u = 0, \quad T' = T_\infty', \quad C' = C_\infty' \quad \text{at } x = 0, \\ u \rightarrow 0, \quad T' \rightarrow T_\infty', \quad C' \rightarrow C_\infty' \quad \text{as } y \rightarrow \infty. \end{aligned} \tag{2.5}$$

On introducing the following non-dimensional quantities

$$\begin{aligned} X = \frac{x}{L}, \quad Y = \frac{y}{L} Gr_L^{1/4}, \quad U = \frac{uL}{\nu} Gr_L^{-1/2}, \quad V = \frac{vL}{\nu} Gr_L^{-1/4}, \quad t = \frac{\nu t'}{L^2} Gr_L^{1/2}, \\ T = \frac{T' - T_\infty'}{T_w'(L) - T_\infty'}, \quad C = \frac{C' - C_\infty'}{C_w'(L) - C_\infty'}, \quad Gr_L = \frac{g\beta L^3 (T_w'(L) - T_\infty')}{\nu^2}, \\ Gr_L^* = \frac{g\beta L^3 (C_w'(L) - C_\infty')}{\nu^2}, \quad Pr = \frac{\nu}{\alpha}, \quad S = \frac{\nu}{D}, \quad N = \frac{Gr_L^*}{Gr_L}, \quad K = \frac{K'L^2}{\nu} Gr_L^{-1/2}. \end{aligned} \tag{2.6}$$

Governing equations reduce to the following form

$$\frac{\partial U}{\partial X} + \frac{\partial V}{\partial Y} = 0, \quad (2.7)$$

$$\begin{aligned} \frac{\partial U}{\partial t} + U \frac{\partial U}{\partial X} + V \frac{\partial U}{\partial Y} = \\ = Gr_L^{-1/4} \cos \phi \frac{\partial}{\partial X} \int_Y^\infty T dY + N Gr_L^{-1/4} \cos \phi \frac{\partial}{\partial X} \int_Y^\infty C dY + T \sin \phi + NC \sin \phi + \frac{\partial^2 U}{\partial Y^2}, \end{aligned} \quad (2.8)$$

$$\frac{\partial T}{\partial t} + U \frac{\partial T}{\partial X} + V \frac{\partial T}{\partial Y} = \frac{1}{Pr} \frac{\partial^2 T}{\partial Y^2}, \quad (2.9)$$

$$\frac{\partial C}{\partial t} + U \frac{\partial C}{\partial X} + V \frac{\partial C}{\partial Y} = \frac{1}{Sc} \frac{\partial^2 C}{\partial Y^2} - KC. \quad (2.10)$$

The corresponding initial and boundary conditions in a dimensionless form are given by

$$t \leq 0: \quad U = 0, \quad V = 0, \quad T = 0, \quad C = 0 \quad \text{for all } X \quad \text{and } Y,$$

$$t > 0: \quad U = 0, \quad V = 0, \quad T = X^n, \quad C = X^m \quad \text{at } Y = 0,$$

$$U = 0, \quad T = 0, \quad C = 0 \quad \text{at } X = 0,$$

$$U \rightarrow 0, \quad T \rightarrow 0, \quad C \rightarrow 0 \quad \text{as } Y \rightarrow \infty. \quad (2.11)$$

### 3. Numerical techniques

The governing Eqs (2.7) – (2.10) represent a coupled system of non-linear integro partial differential equations, which are solved numerically under the initial and boundary conditions (2.11) using the Crank-Nicolson implicit finite difference scheme. The finite difference equations corresponding to Eqs (2.7) – (2.10) are as follows

$$\begin{aligned} \frac{[U_{i,j}^{m+1} - U_{i-1,j}^{m+1} + U_{i,j}^m - U_{i-1,j}^m + U_{i,j-1}^{m+1} - U_{i-1,j-1}^{m+1} + U_{i,j-1}^m - U_{i-1,j-1}^m]}{4\Delta X} + \\ + \frac{[V_{i,j}^{m+1} - V_{i,j-1}^{m+1} + V_{i,j}^m - V_{i,j-1}^m]}{2\Delta Y} = 0, \end{aligned} \quad (3.1)$$

$$\begin{aligned} \frac{[U_{i,j}^{m+1} - U_{i,j}^m]}{\Delta t} + U_{i,j}^m \frac{[U_{i,j}^{m+1} - U_{i-1,j}^{m+1} + U_{i,j}^m - U_{i-1,j}^m]}{2\Delta X} + V_{i,j}^m \frac{[U_{i,j+1}^{m+1} - U_{i,j-1}^{m+1} + U_{i,j+1}^m - U_{i,j-1}^m]}{4\Delta Y} = \\ = Gr_L^{-1/4} \cos \phi \frac{\partial}{\partial X} \int_Y^\infty T dY + N Gr_L^{-1/4} \cos \phi \frac{\partial}{\partial X} \int_Y^\infty C dY + \frac{1}{2} [T_{i,j}^{m+1} + T_{i,j}^m] \sin \phi + \frac{N}{2} [C_{i,j}^{m+1} + C_{i,j}^m] \sin \phi + \\ + \frac{[U_{i,j-1}^{m+1} - 2U_{i,j}^{m+1} + U_{i,j+1}^{m+1} + U_{i,j-1}^m - 2U_{i,j}^m + U_{i,j+1}^m]}{2(\Delta Y)^2}, \end{aligned} \quad (3.2)$$

$$\begin{aligned} & \frac{[T_{i,j}^{m+1} - T_{i,j}^m]}{\Delta t} + U_{i,j}^m \frac{[T_{i,j}^{m+1} - T_{i-1,j}^{m+1} + T_{i,j}^m - T_{i-1,j}^m]}{2\Delta X} + \\ & + V_{i,j}^m \frac{[T_{i,j+1}^{m+1} - T_{i,j-1}^{m+1} + T_{i,j+1}^m - T_{i,j-1}^m]}{4\Delta Y} = \frac{I}{Pr} \frac{[T_{i,j-1}^{m+1} - 2T_{i,j}^{m+1} + T_{i,j+1}^{m+1} + T_{i,j-1}^m - 2T_{i,j}^m + T_{i,j+1}^m]}{2(\Delta Y)^2}, \end{aligned} \quad (3.3)$$

$$\begin{aligned} & \frac{[C_{i,j}^{m+1} - C_{i,j}^m]}{\Delta t} + U_{i,j}^m \frac{[C_{i,j}^{m+1} - C_{i-1,j}^{m+1} + C_{i,j}^m - C_{i-1,j}^m]}{2\Delta X} + \\ & + V_{i,j}^m \frac{[C_{i,j+1}^{m+1} - C_{i,j-1}^{m+1} + C_{i,j+1}^m - C_{i,j-1}^m]}{4\Delta Y} = \frac{I}{Sc} \frac{[C_{i,j-1}^{m+1} - 2C_{i,j}^{m+1} + C_{i,j+1}^{m+1} + C_{i,j-1}^m - 2C_{i,j}^m + C_{i,j+1}^m]}{2(\Delta Y)^2}. \end{aligned} \quad (3.4)$$

The domain of integration is considered as a rectangle with sides  $X_{\max} (= I)$  and  $Y_{\max} (= I6)$ , where  $Y_{\max}$  corresponds to  $Y = \infty$ , which lies very well outside the momentum, energy and concentration boundary layers. The maximum of  $Y$  was chosen as 16 after some preliminary investigations so that the last two of the boundary conditions (2.11) are satisfied. At an arbitrary time step, the coefficients  $U_{i,j}^m$  and  $V_{i,j}^m$  appearing in the difference equations are treated as constants. The values of  $U$ ,  $V$ ,  $T$  and  $C$  are known at all grid points at  $t = 0$ , from the initial conditions. The computations of  $U$ ,  $V$ ,  $T$  and  $C$  at time level  $(m + 1)$  using the values at previous time level  $(m)$  are carried out as follows: The finite difference Eq.(3.4) at every internal nodal point on a particular  $i$ -level constitutes a tridiagonal system of equations. Such systems of equations are solved by Thomas algorithm as described in Carnahan *et al* [15]. Thus, the values of  $C$  are found at every nodal point for a particular  $I$  at  $(m + 1)^{\text{th}}$  time level. Similarly, the values of  $T$  are calculated from Eq.(3.3). Using the values of  $C$  and  $T$  at  $(m + 1)^{\text{th}}$  time level in Eq.(3.2), the values of  $U$  at  $(m + 1)^{\text{th}}$  time level are found in a similar manner. Thus, the values of  $T$  and  $U$  are known on a particular  $i$ -level. Finally, the values of  $V$  are calculated explicitly using Eq.(3.1) at every nodal point on a particular  $i$ -level at  $(m+1)^{\text{th}}$  time level. This process is repeated for various  $i$ -levels. Thus the values of  $T$ ,  $U$  and  $V$  are known, at all grid points in the rectangular domain at  $(m + 1)^{\text{th}}$  time level.

Computations are carried out until the steady-state is reached. The steady-state solution is assumed to have been reached, when the absolute difference between the values of  $U$ , as well as temperature  $T$  and concentration  $C$  at two consecutive time steps are less than  $10^{-5}$  at all grid points. After experimenting with a few set of mesh sizes, the grid steps were fixed at the level  $\Delta X = 0.05$  and  $\Delta Y = 0.25$ , the time-step size dependency was fixed at  $\Delta t = 0.01$ . When the mesh size is reduced by 50% in the  $X$ -direction, in the  $Y$ -direction and simultaneously in both directions, the results differ in the fourth decimal place.

The local truncation error is  $O(\Delta t^2 + \Delta Y^2 + \Delta X)$  and it tends to zero as  $\Delta t$ ,  $\Delta X$  and  $\Delta Y$  tend to zero, which shows that the scheme is compatible. Also the Crank-Nicolson type of implicit finite difference scheme is unconditionally stable. Thus, compatibility and stability ensures that the implicit finite difference scheme is convergent.

#### 4. Results and discussion

We considered a homogenous first order chemical reaction, hence the chemical reaction parameter  $K$  has the dimensions of the reciprocal of time. The diffusion species either can be destroyed or generated in the homogenous reaction. The mass diffusion Eq.(2.10) can be adjusted to meet these circumstances if one takes

1.  $K > 0$  for the destructive reaction
2.  $K < 0$  for the generative reaction and
3.  $K = 0$  for no reaction.

In order to get a physical insight into the problem, we have computed the numerical values of the velocity, temperature and concentration. Computation has been carried out for different values of the chemical reaction parameter  $K$ , for fluids with the Prandtl number equal to 0.7(air), 7.0(water), for the different inclination angle  $\phi$ , for different values of the exponent  $n$  and  $m$ , for different values of the Grashof number and different values of the Schmidt number.

Temporal maximum and steady state values for different values of the buoyancy ratio parameter  $N$  and the chemical reaction parameter  $K$  for velocity, temperature and concentration are shown in Figs 1-3 respectively. In Fig.1, transient velocity profiles are plotted for different values of the buoyancy ratio parameter  $N$  and chemical reaction parameter  $K$ . An increase in  $N$  leads to an increase in the velocity. This indicates that the buoyancy force due to concentration dominates in the region near the plate over thermal buoyancy force on velocity. But velocity decreases with increasing value of  $N$  somewhere near the region  $Y > 3$ . One can readily observe that the influence of the thermal boundary force on increasing the velocity is larger compared to that of concentration buoyancy force in the region away from the plate. The velocity increases in the case of a generative reaction and decreases in the case of a destructive reaction. The time needed to reach the steady state increases with increasing the chemical reaction parameter  $K$ . From the numerical values, we noticed that the difference between the temporal maximum and steady state decreases as  $K$  increases in the case of a destructive reaction. In Fig.2, transient temperature profiles are plotted for different values of  $N$  and  $K$ . It is observed that the temperature increases with the increasing value of the chemical reaction parameter. Also it is observed that temperature decreases as  $N$  increases. Temporal maximum and steady state values of concentration distribution are given in Fig.3, for different values of  $N$  and  $K$ . The effect of chemical reaction parameter is very important in the concentration field. There is a fall in concentration due to increasing values of the chemical reaction parameter or buoyancy ratio parameter.

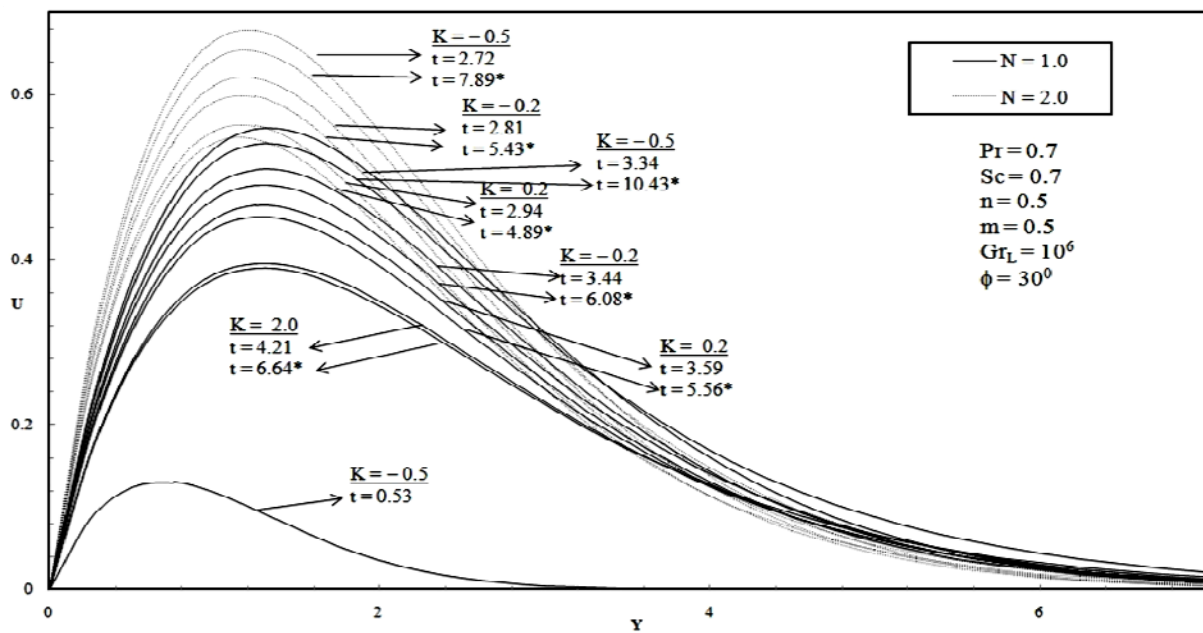


Fig.1. Transient velocity profiles at  $X=1.0$  for different  $N$  and  $K$  (\*- steady state).

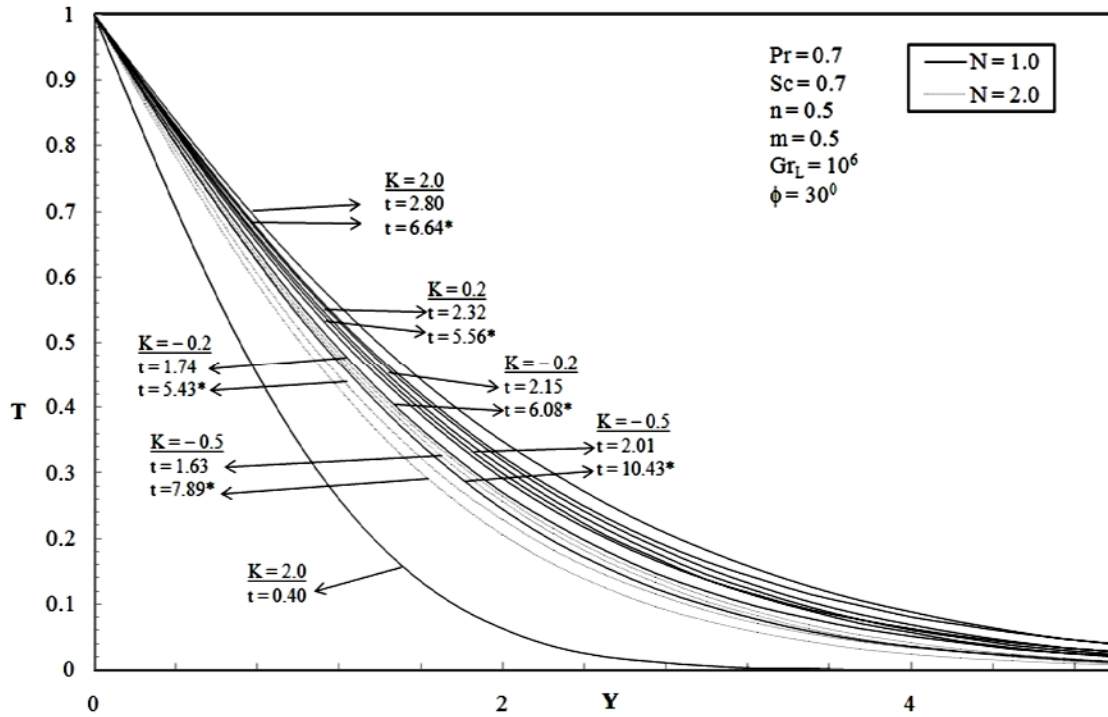


Fig.2. Transient temperature profiles at  $X=1.0$  for different  $N$  and  $K$  (\*- steady state).

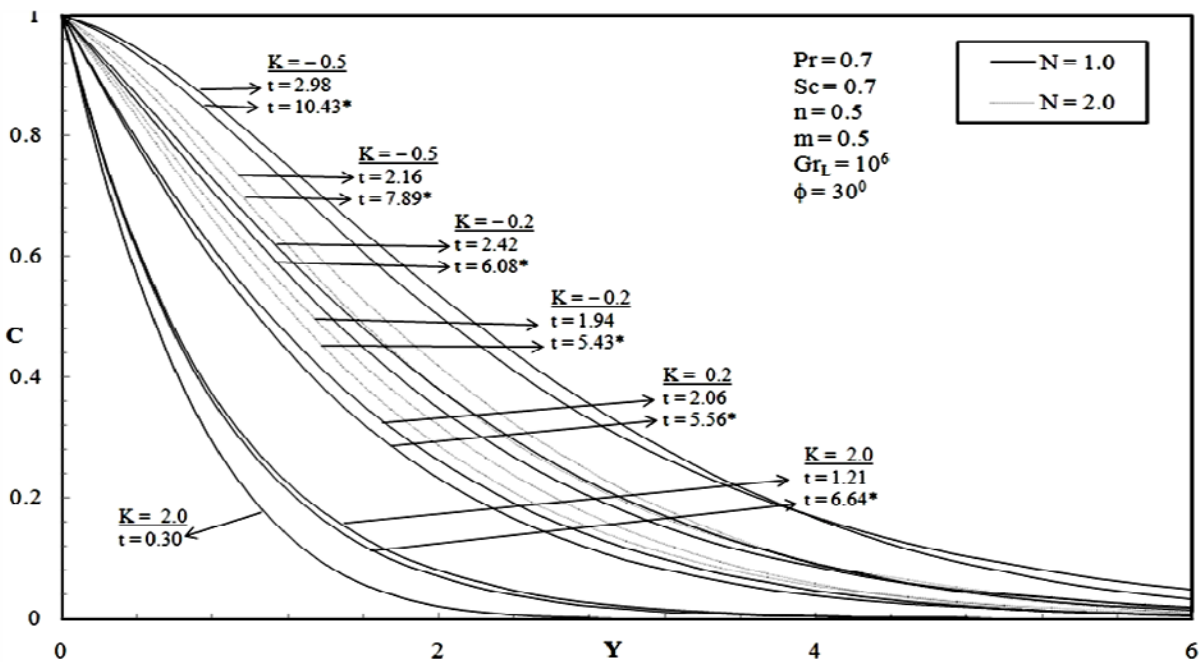


Fig.3. Transient concentration profiles at  $X=1.0$  for different  $N$  and  $K$  (\*- steady state).

Figures 4-6 show the temporal maximum and steady state velocity, temperature and concentration profiles for different values of the Grashof number  $Gr_L$  and the inclination angle  $\phi$  respectively. In Fig.4, we observed that the velocity increases steadily and reaches a steady state after some time. Since the tangential component of the buoyancy force increases with  $\phi$  and dominates in the down stream, higher velocity is

experienced throughout the transient period as well as in the steady state level for a system having larger angles of inclination. The velocity of air ( $Pr=0.7$ ) decreases with increasing the Grashof number throughout the transient period. It is observed that the temperature decreases as the angle of inclination  $\phi$  increases. Also, it is noticed that the system reaches steady state quickly when  $\phi$  increases. From the calculated numerical results we noticed that the temperatures decreases as the Grashof number increases. It is also observed that concentration is lower for systems with larger values of  $\phi$ . The effect of the Grashof number on concentration is nil.

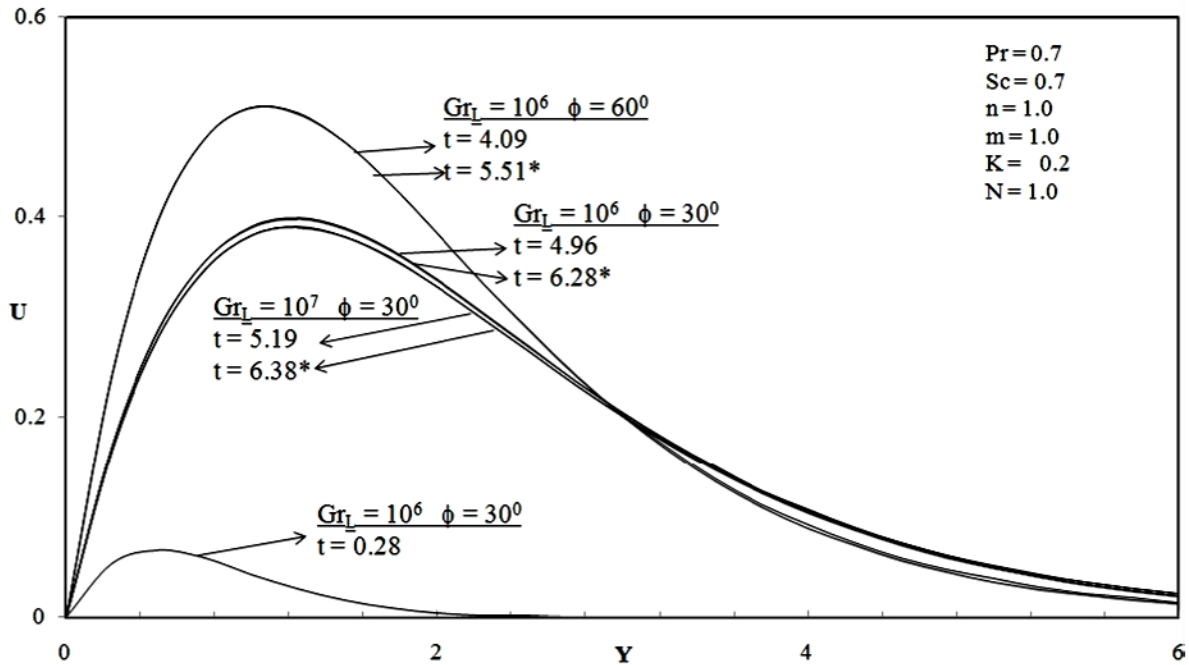


Fig.4. Transient velocity profiles at  $X=1.0$  for different  $Gr_L$  and  $\phi$  (\*- steady state).

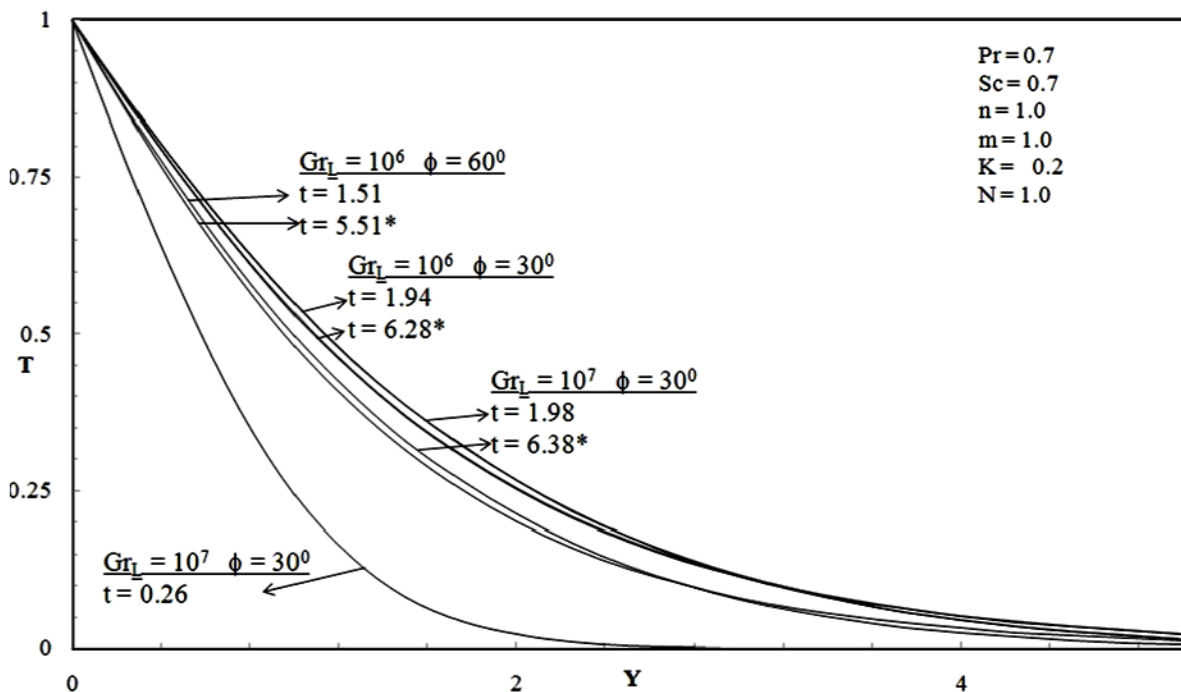


Fig.5. Transient temperature profiles at  $X=1.0$  for different  $Gr_L$  and  $\phi$  (\*- steady state).

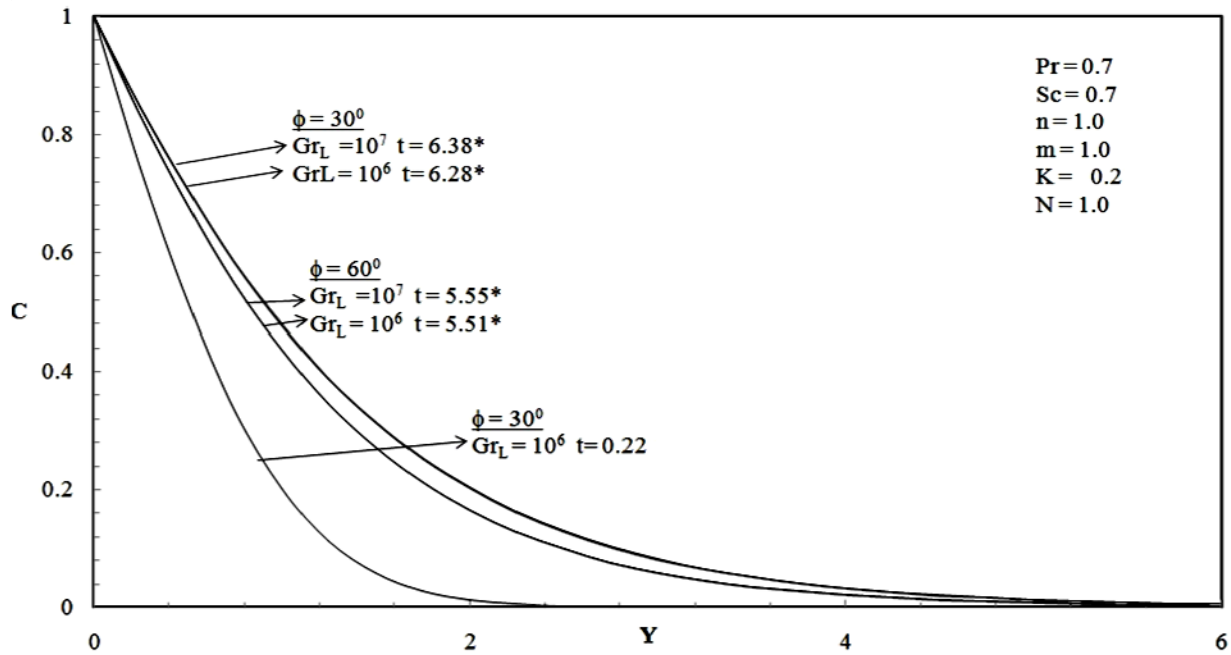


Fig.6. Transient concentration profiles at  $X=1.0$  for different  $\text{Gr}_L$  and  $\phi$  (\*- steady state).

The effects of exponent  $n$  and  $m$  on transient velocity, temperature and concentration distribution near the plate at  $X = 1.0$  are presented in Figs 7-9, respectively. The increase in the value of  $n$  and  $m$  reduces velocity on the surface up to the height of the plate  $X = 1.0$ . Therefore velocity decreases with increasing the value of  $n$  or  $m$ . The difference between the temporal maximum and steady state decreases with the increasing value of exponent  $m$ . According to the numerical result, the system reaches the steady state quickly when  $n = m$  as opposed to with  $n < m$ . Also, we observed that the temperature distribution decreases as exponent  $n$  or  $m$  increases. It is observed that concentration reduces with increasing the value of  $n$  or  $m$ .

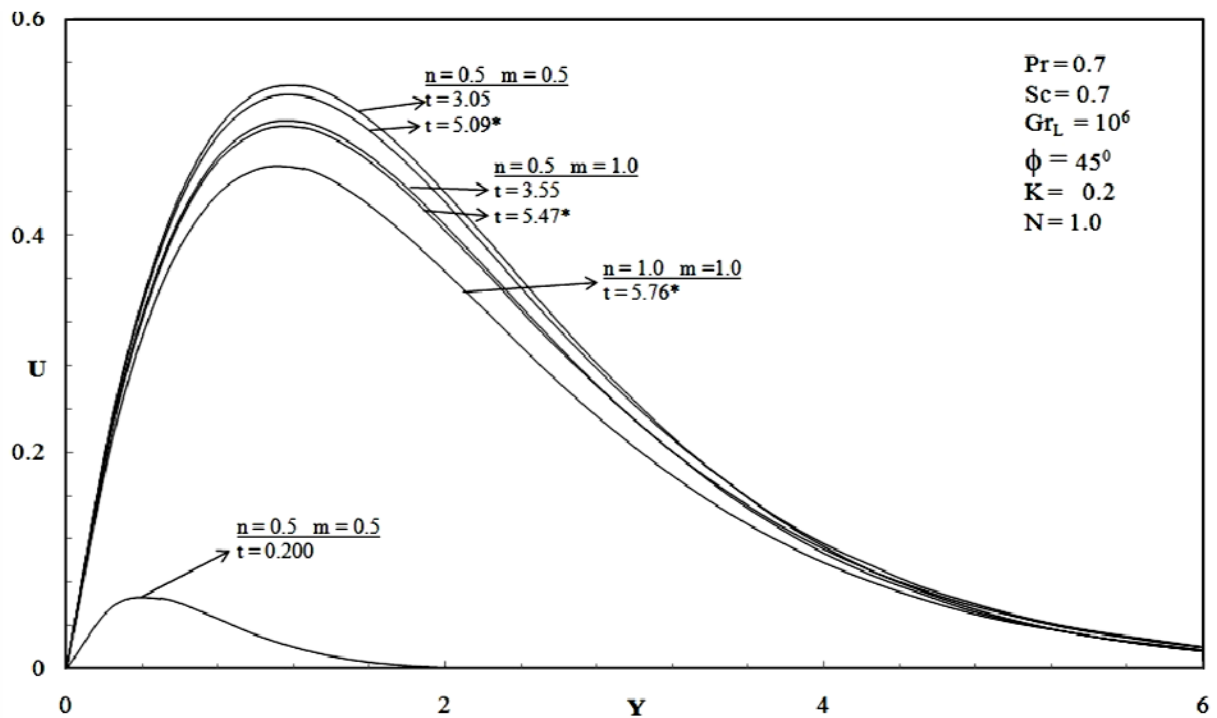


Fig.7. Transient velocity profiles at  $X=1.0$  for different  $n$  and  $m$  (\*-steady state).

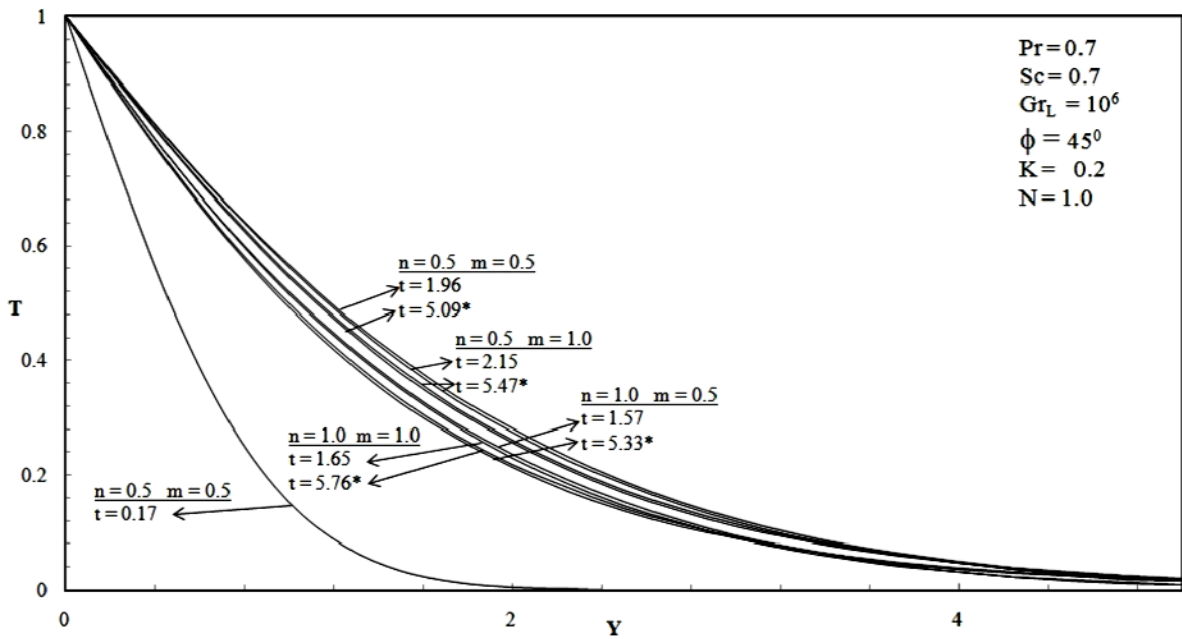


Fig.8. Transient temperature profiles at  $X=1.0$  for different  $n$  and  $m$  (\*-steady state).

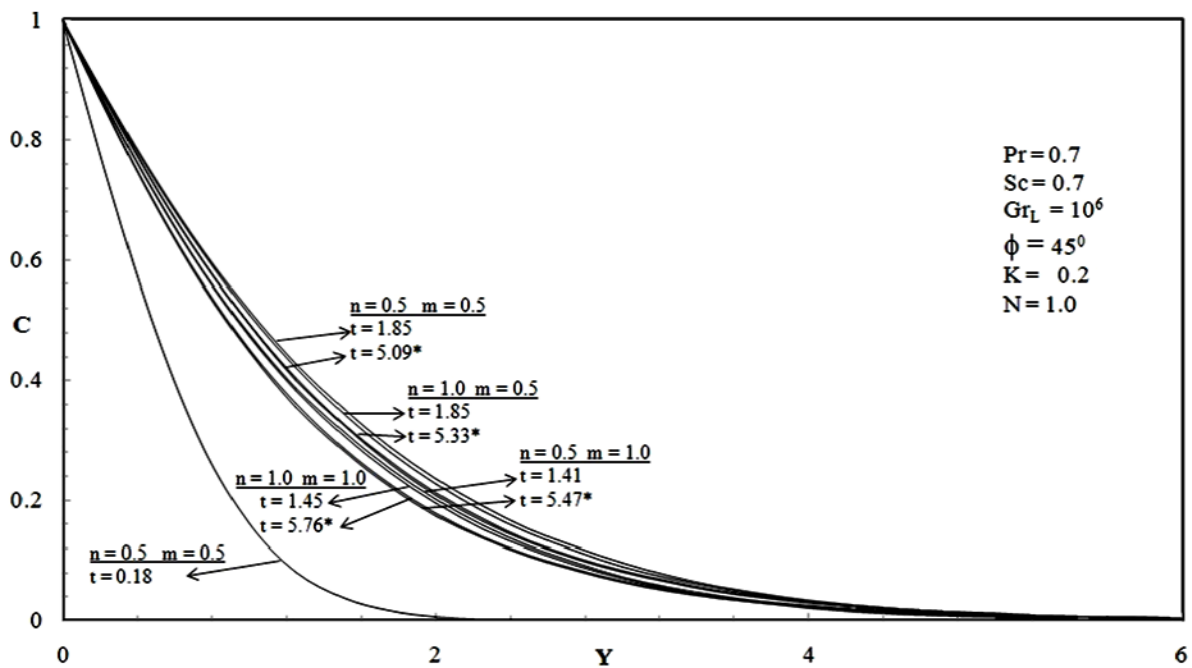


Fig.9. Transient concentration profiles at  $X=1.0$  for different  $n$  and  $m$  (\*-steady state).

For various values of the Schmidt number and Prandtl number, transient velocity profiles are plotted in Fig.10. We observe that there is a decrease in the velocity as Pr increases, i.e., for  $Pr = 0.7$  (air),  $0.7$  (water). An increase in Sc leads to a fall in the velocity. Time taken to reach the steady state increases as Sc increases irrespective of the Prandtl number of the fluid. The difference between the temporal maximum and steady state velocity decreases as Sc increases.

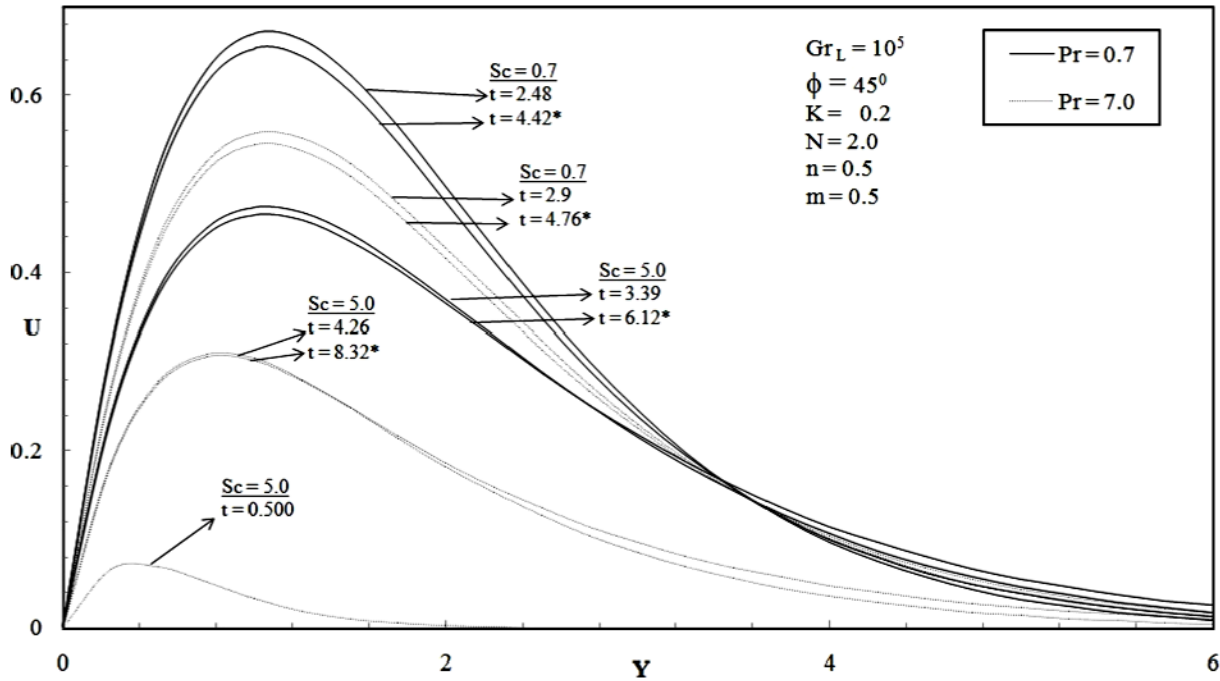


Fig.10. Transient velocity profiles at  $X=1.0$  for different Pr and Sc (\*-steady state).

Transient temperature profiles for different values of Pr and Sc are shown in Fig.11. The effect of the Prandtl number is very important in the temperature profiles. Larger Pr values give rise to thicker temperature profiles, since increasing Pr values give rise to increasing heat transfer. Lower temperature is experienced in a system of lower values of Sc.

The effects of Schmidt and Prandtl number on transient concentration profiles are shown in Fig.12. Concentration increases with increasing the Prandtl number whereas it decreases with increasing the Schmidt number.

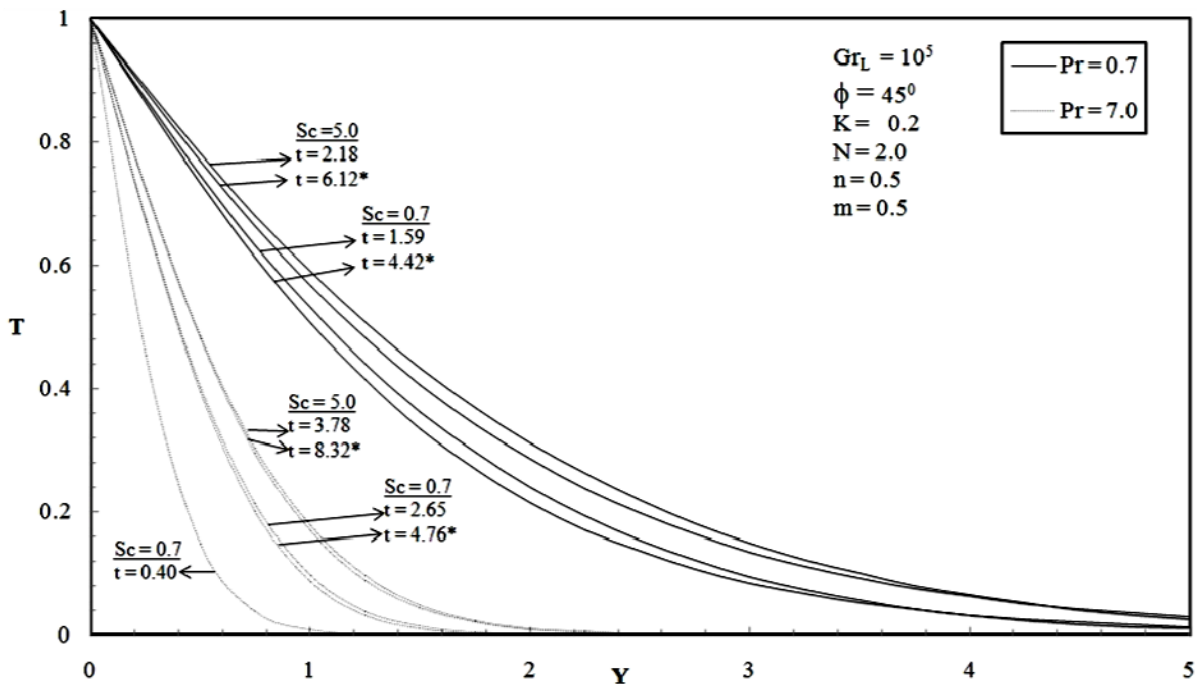


Fig.11. Transient temperature profiles at  $X=1.0$  for different Pr and Sc (\*-steady state).

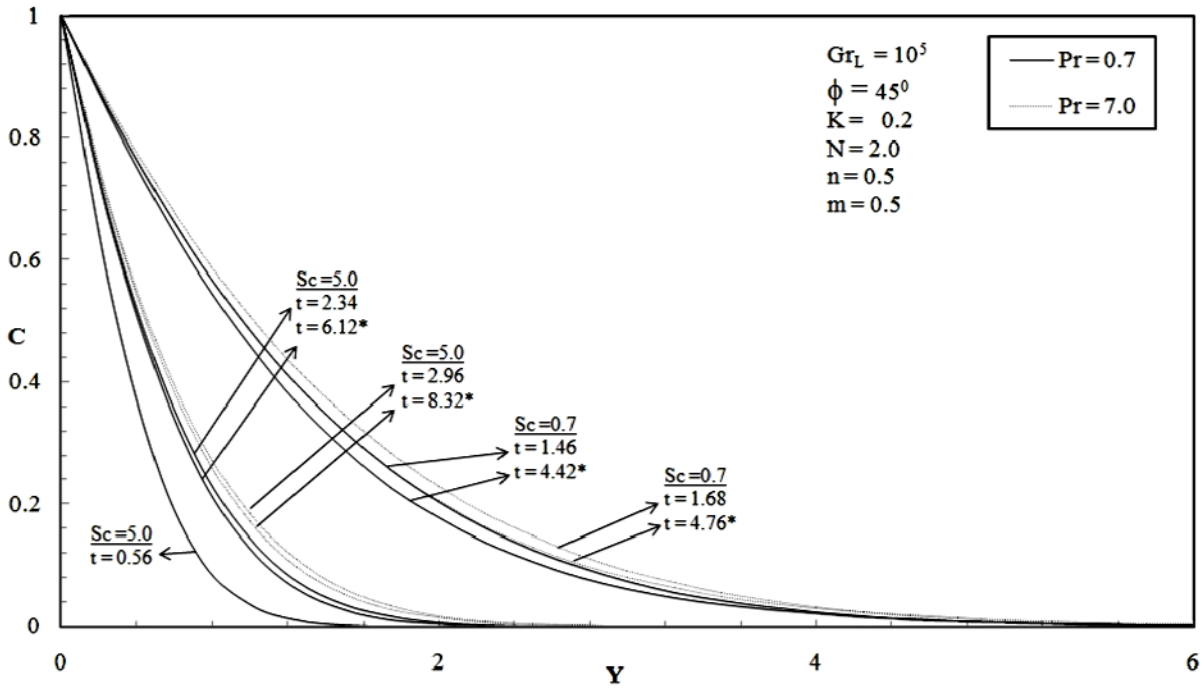


Fig.12. Transient concentration profiles at  $X=1.0$  for different Pr and Sc (\*-steady state).

We now study the local and average skin friction, local and average Nusselt number, local and average Sherwood number. In non-dimensional quantities, they are given by

$$\tau_X = Gr_L^{3/4} \left( \frac{\partial U}{\partial Y} \right)_{Y=0}, \tag{4.1}$$

$$\bar{\tau} = Gr_L^{3/4} \int_0^1 \left( \frac{\partial U}{\partial Y} \right)_{Y=0} dX, \tag{4.2}$$

$$Nu_X = \frac{XGr_L^{1/4}}{T_{Y=0}} \left( -\frac{\partial T}{\partial Y} \right)_{Y=0}, \tag{4.3}$$

$$\bar{Nu} = -Gr_L^{1/4} \int_0^1 \frac{\left( \frac{\partial T}{\partial Y} \right)_{Y=0}}{T_{Y=0}} dX, \tag{4.4}$$

$$Sh_X = \frac{XGr_L^{1/4}}{C_{Y=0}} \left( -\frac{\partial C}{\partial Y} \right)_{Y=0}, \tag{4.5}$$

$$\bar{Sh} = -Gr_L^{1/4} \int_0^1 \frac{\left( \frac{\partial C}{\partial Y} \right)_{Y=0}}{C_{Y=0}} dX. \tag{4.6}$$

The derivatives involved in Eqs (4.1) to (4.6) are evaluated by using a five-point approximation formula and then the integrals are evaluated by the Newton-Cotes closed integration formula.

In Fig.13, values of the local shear stress are plotted for various values of the buoyancy ratio parameter  $N$ , chemical reaction parameter  $K$ , exponent  $n$  and  $m$ . local skin friction increases as  $X$  increases. The local wall shear stress decreases during a destructive reaction. The Local skin friction increases with the increasing value of  $N$ , because velocity increases with the increasing value of  $N$  as shown in Fig.1. It is observed that by increasing  $n$  or  $m$ , skin friction can be reduced.

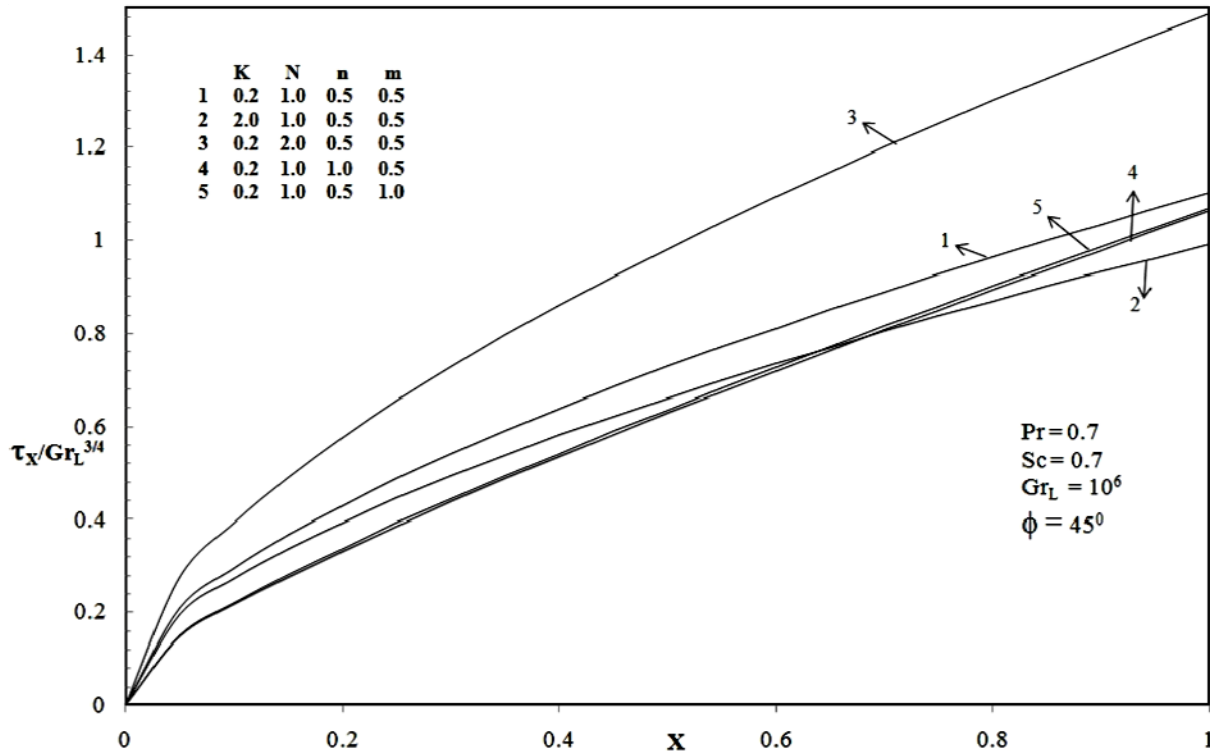


Fig.13. Lokal skin friction.

Values of the local Nusselt number for different values of  $K$ ,  $N$ ,  $n$  and  $m$  are shown in Fig.14. As the buoyancy ratio parameter increases, a higher value of the Nusselt number is observed. The rate of heat transfer decreases with increasing the value of  $K$  during a destructive reaction. It is observed that the local Nusselt number increases as  $n$  increases. But it decreases as  $m$  increases.

Values of the local Sherwood number are plotted in Fig.15 at steady state. They increase as the axial co-ordinate  $X$  increases. For the buoyancy ratio parameter, the local Sherwood number increases as  $N$  or  $m$  increases. The rate of concentration distribution increases as  $K$  increases during a destructive reaction. The Local Sherwood number decreases as  $n$  increases.

The effect of the chemical reaction parameter  $K$ , buoyancy ratio parameter  $N$ , exponent  $n$  and  $m$  on average skin friction, the Nusselt number and the Sherwood number are shown in Figs 16, 17 and 18 respectively. In Fig.16, it is observed that skin friction increases with time and reaches a steady state after some lapse of time. Average skin friction increases with  $N$  throughout the transient period and at steady state level. For a destructive reaction skin friction is reduced for increasing value of  $K$  is noticed. Average skin friction decreases with increasing  $n$  or  $m$ . The average Nusselt number is found to increase with increasing the value of  $N$  or  $n$ . The Average Nusselt number decreases as  $K$  increases in the case of a destructive reaction. Also, we observed that the average Nusselt number decreases as  $m$  increases. We observe from Fig.18 that the behavior of average Sherwood Number is the same as the local Sherwood number with

respect to  $N$  and  $K$ . The Average Sherwood number is independent of time when  $t$  is large. The Average Sherwood number decreases as  $n$  increases, but it increases as  $m$  increases.

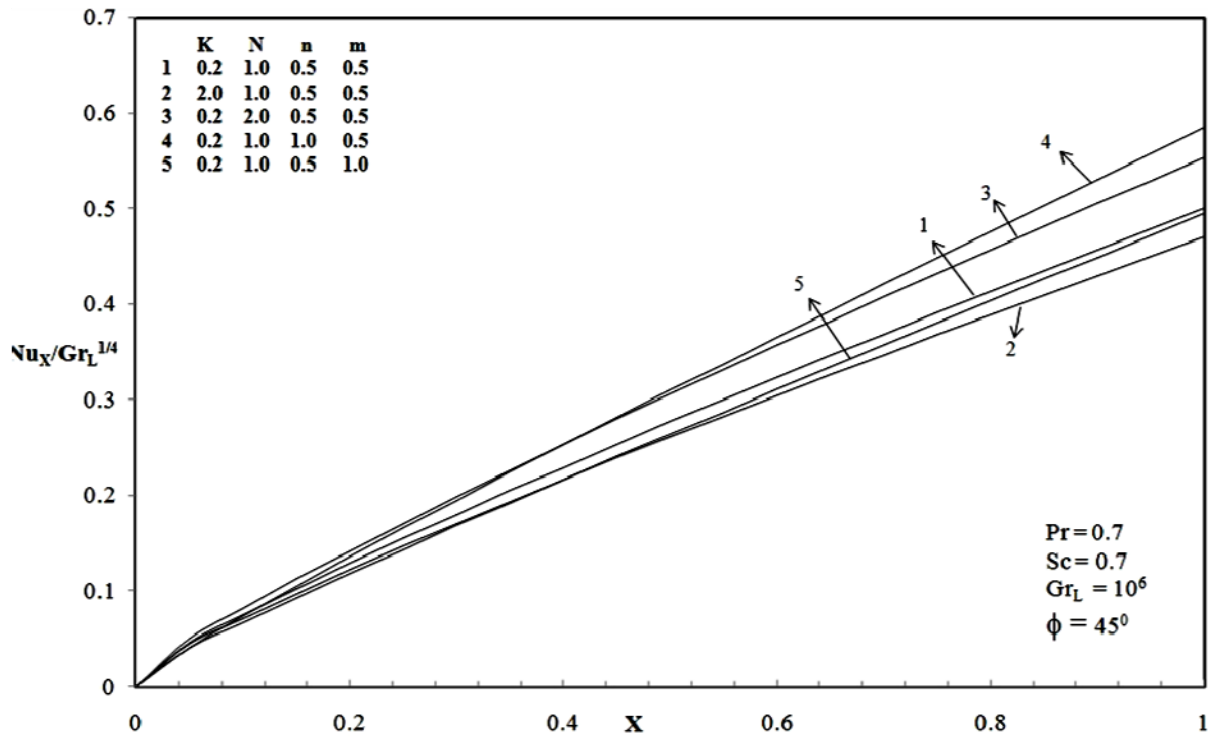


Fig.14. Local Nusselt number.

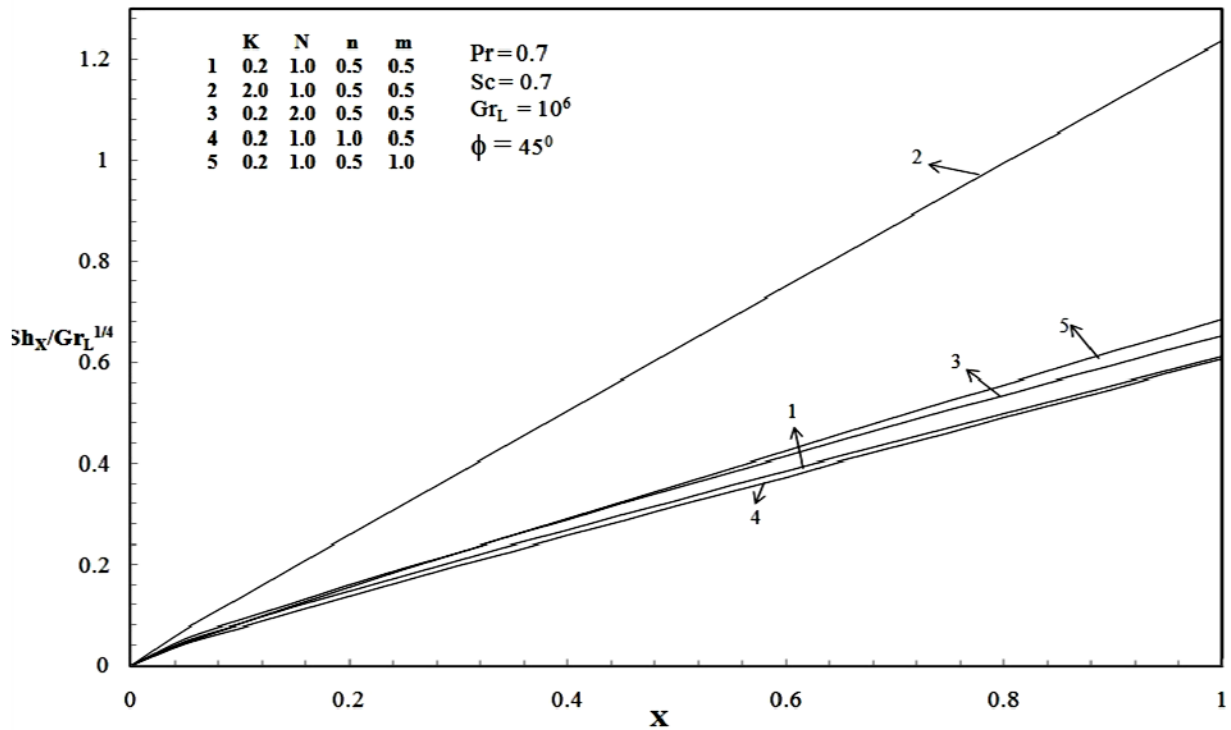


Fig.15. Local Sherwood number.

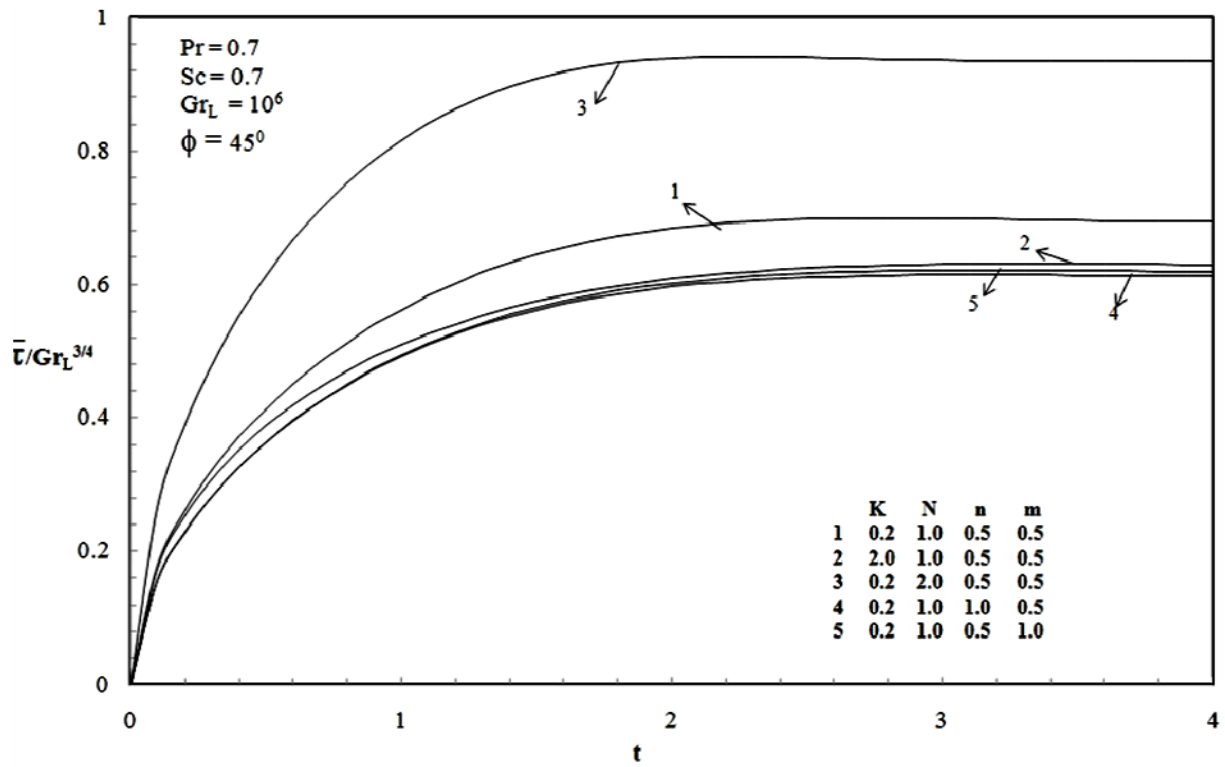


Fig.16. Average skin friction.

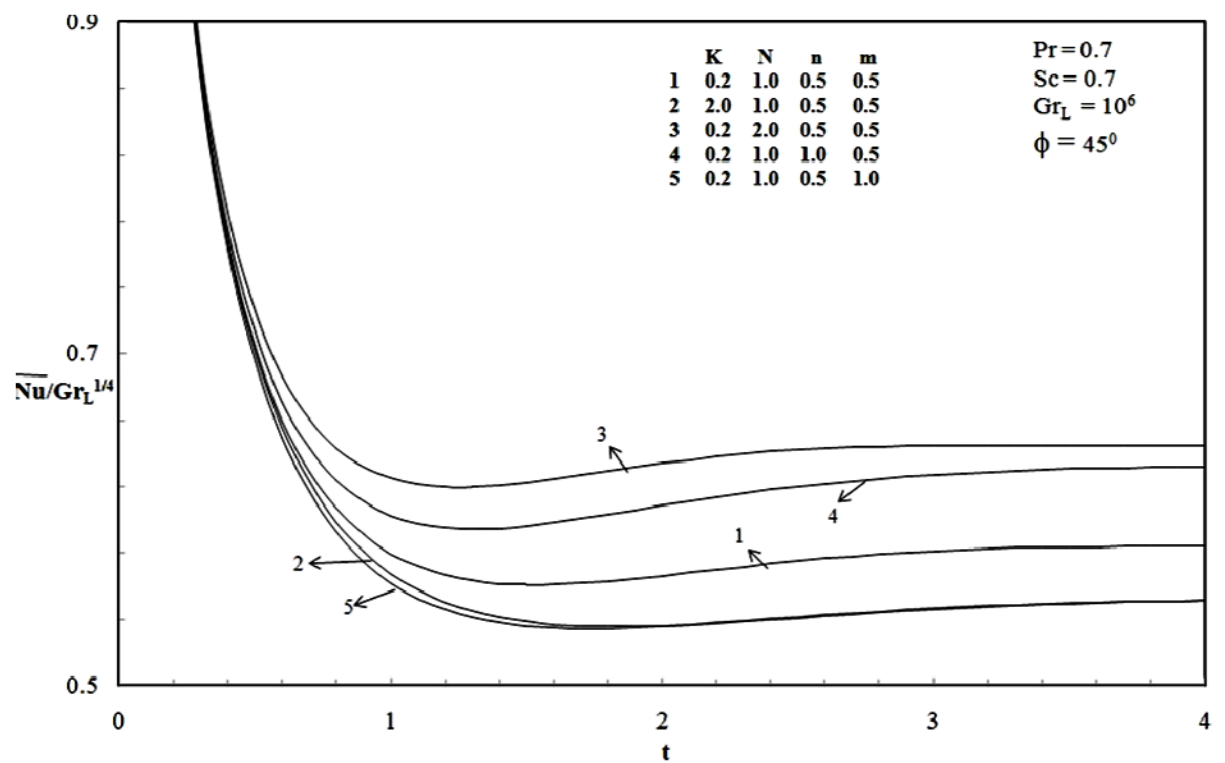


Fig.17. Average Nusselt number.

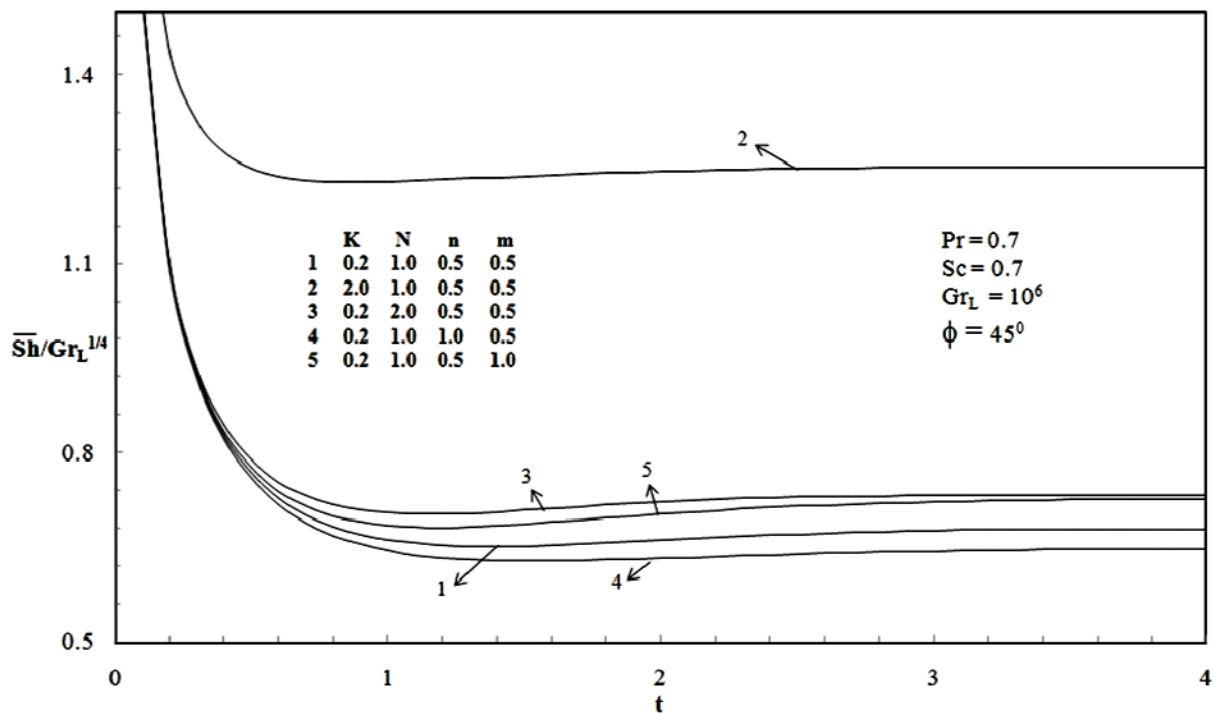


Fig.18. Average Sherwood number.

## 5. Conclusions

A detailed numerical study has been carried out for a chemically reactive flow past a semi-infinite inclined plate with variable surface temperature and variable mass diffusion. The dimensionless governing equations are solved by an efficient finite-difference method of Crank –Nicolson type. The conclusion of this study is as follows:

1. The velocity increases in the case of generative reaction and decreases in the case of a destructive reaction.
2. The difference between the temporal maximum and steady state decreases as  $K$  increases in the case of a destructive reaction.
3. The system reaches the steady state quickly when  $n = m$  as opposed to  $n < m$ .
4. The local wall shear stress decreases during a destructive reaction.
5. The rate of concentration distribution increases as  $K$  increases during a destructive reaction.

## Nomenclature

- $C$  – dimensionless species concentration  
 $C'$  – species concentration  
 $D$  – coefficient of diffusion in the mixture  
 $Gr_L$  – thermal Grashof number at  $X = L$   
 $Gr_L^*$  – mass Grashof number at  $X = L$   
 $g$  – acceleration due to gravity  
 $K$  – dimensionless chemical reaction parameter  
 $K'$  – chemical reaction parameter  
 $L$  – characteristic length  
 $m$  – exponent in the power law variation of the concentration on the wall

- $N$  – buoyancy ratio parameter  
 $\overline{Nu}$  – dimensionless average Nusselt number  
 $Nu_x$  – dimensionless local Nusselt number  
 $n$  – exponent in the power law variation of the wall temperature  
 $Pr$  – Prandtl number  
 $Sc$  – Schmidt number  
 $\overline{Sh}$  – dimensionless average Sherwood number  
 $Sh_x$  – dimensionless local Sherwood number  
 $T$  – dimensionless temperature  
 $T$  – temperature of fluid away from the plate  
 $T_w$  – temperature of the plate  
 $T'$  – temperature  
 $t$  – dimensionless time  
 $t'$  – time  
 $U, V$  – dimensionless velocity components in the  $X, Y$  directions respectively  
 $u, v$  – velocity components in the  $x, y$  directions respectively  
 $X$  – dimensionless spatial coordinate along the plate  
 $x$  – spatial coordinate along the plate  
 $Y$  – dimensionless spatial coordinate normal to the plate  
 $y$  – spatial coordinate normal to the plate  
 $\alpha$  – thermal diffusivity  
 $\beta$  – volumetric coefficient of thermal expansion  
 $\beta^*$  – volumetric coefficient of expansion with concentration  
 $\nu$  – kinematic velocity  
 $\tau_x$  – local skin friction  
 $\overline{\tau}$  – average skin friction  
 $\phi$  – angle of inclination with the horizontal

### Subscripts

- $w$  – conditions at the wall  
 $\infty$  – free stream conditions

### References

- [1] Somers E.V. (1956): *Theoretical considerations of combined thermal and mass transfer from a vertical flat plate.* – J. Appl. Mech., vol.23, pp.295-301.  
 [2] Mathers W.G., Madden A.J. and Piret E.L. (1957): *Simultaneous heat and mass transfer in free convection.* – Ind. Engng. Chem., vol.49, pp.961-968.  
 [3] Wilcox W.R. (1961): *Simultaneous heat and mass transfer in free convection.* – Chem. Engng. Sci., vol.13, pp.113-119.  
 [4] Gebhart B. and Pera L. (1971): *The nature of vertical natural convection flows resulting from combined buoyancy effects of thermal and mass diffusion.* – Int. J. Heat Mass Trans., vol.14, pp.2025-2050.  
 [5] Callahan G.D. and Marner W.J. (1970): *Transient free convection with mass transfer on an isothermal vertical flat plate.* – Int. J. Heat Mass Trans., vol.19, pp.165-174.  
 [6] Ekanbavannan K. and Ganesan P. (1995): *Finite difference analysis of unsteady natural convection along an inclined plate with variable surface temperature and mass diffusion.* – Heat and Mass Transfer, vol.31, pp.17-24.  
 [7] Chambre P.L. and Young J.D. (1958): *On the diffusion of a chemically reactive species in laminar boundary layer flow.* – Physics of Fluids, vol.1, pp.48-54.

- [8] Das U.N., Deka R.K. and Soundalgekar V.M. (1994): *Effects of mass transfer on flow past an impulsively started infinite vertical plate with constant heat flux and chemical reaction.* – Engineering Research, vol.60, pp.284-287.
- [9] Das U.N., Deka R.K. and Soundalgekar V.M. (1994): *Effects of mass transfer on flow past an impulsively started infinite vertical plate with chemical reaction.* – Engineering Research, vol.60, pp.284-287.
- [10] Muthucumaraswamy R. and Ganesan P. (2000): *On impulsive motion of a vertical plate with heat flux and diffusion of chemically reactive species.* – Forsch. Ingenieurw, vol.66, pp.17-23.
- [11] Muthucumaraswamy R. and Ganesan P. (2002): *Diffusion and first order chemical reaction on impulsively started infinite vertical plate with variable temperature.* – Int. J. Thermal Sci., vol.41, pp.475-479.
- [12] Anjali Devi S.P. and Kandsamy R. (2003): *Effects of chemical reaction, heat and mass transfer on non-linear MHD flow over an accelerating surface with heat source and thermal stratification in the presence of suction or injection.* – Comm. Numer. Methods Engg., vol.1, pp.513-520.
- [13] Muthucumaraswamy R. and Kulandaivel T. (2003): *Chemical reaction effects on moving infinite vertical plate with uniform heat flux and variable mass diffusion.* – Forsch, Ingenieurw, vol.68, pp.101-104.
- [14] Loganathan P., Kulandaivel T. and Muthucumaraswamy R. (2008): *First order chemical reaction on moving semi-infinite vertical plate in the presence of optically thin gray gas.* – Int. J. Appl. Math. Mech., vol.4, No.5, pp.26-41.
- [15] Carnahan B., Luther H.A. and Wilkes J.O. (1969): *Applied Numerical Methods.* – New York: John Wiley and Sons.

Received: December 5, 2015

Revised: May 25, 2016